

## Rapid Communication

Martin Buchholz, Ingo Spahn\*, and Heinz H. Coenen

# Optimized separation procedure for production of no-carrier-added radiomanganese for positron emission tomography

DOI 10.1515/ract-2015-2506

Received September 4, 2015; accepted October 12, 2015; published online November 4, 2015

**Abstract:** The  $^{nat}\text{Cr}(p, xn)$ -process is a very efficient route for production of  $^{52g}\text{Mn}$  ( $T_{1/2} = 5.59$  d). Based on measurements of distribution coefficients with different media and ion-exchange resins, an optimized chromatographic separation of radiomanganese from  $^{nat}\text{Cr}$  with the resin Amberlite CG400 was developed. With this system  $^{nat}\text{Cr}$  is eluted first with an acetic acid/methanol 1 : 1 mixture at room temperature and  $^{52g}\text{Mn}$  thereafter with 3 M HCl at 50 °C. Within a separation time of 4 h the method yielded 99.5% of the n.c.a.  $^{52g}\text{Mn}$  in 2–3 mL of 3 M HCl. An ICP-MS analysis revealed a chromium impurity of 0.07 mg (0.014%) in the n.c.a.  $^{52g}\text{Mn}$  solution, making this separation method suitable for the production of  $^{52g}\text{Mn}$  for medical applications like positron emission tomography (PET).

**Keywords:** Radiomanganese,  $^{51,52m,52g}\text{Mn}$ , non-standard PET nuclides, radiochemical separation, ion exchange chromatography.

## 1 Introduction

The natural mono-isotopically occurring  $^{55}\text{Mn}$  is an essential trace element in the mammalian body and is currently increasingly used in animal research studies with Manganese Enhanced Magnetic Resonance Imaging (MEMRI). The divalent manganese ion can enter neuronal cells *via* voltage gated calcium channels and is in addition a strong  $T_1$  contrast enhancing agent. Due to its increased uptake

in excited nerve cells it can be used for the visualization of neuronal activity in the heart and especially in the brain. In the case of brain imaging, it enables tracing the neuronal pathways and even displaying the complete cytoarchitecture after systemic dose application by MEMRI in animals [1–4]. However, high doses of free manganese cations have neurotoxic effects in the brain and may lead to symptoms similar to Parkinson's disease [5]. Therefore, MEMRI operates normally at the lowest mass of contrast agent possible [3, 4, 6–8], but has still not been approved for application in humans. Its use for bi-modal PET/MR-imaging might be a valuable evaluation tool, bringing this method closer to human application.

The introduction of nuclear imaging methods can deliver reliable *in vivo* distribution data for the evaluation of new contrast agents at extremely low concentrations. In order to realise a quantitation of such bi-modal agents, several PET radioisotopes ( $^{18}\text{F}$ ,  $^{68}\text{Ga}$ , etc.) are considered for labelling purposes. Unfortunately, all of those lead to a change of the original molecular composition of the labelled imaging agent. The outcome may thus be an altered *in vivo* behaviour due to a deviating chemical composition, structure and/or coordination, hydration sphere or lipophilicity which would neglect the effort of providing a chemical analogue with an identical distribution in the body. An isotopic labelling with a suitable PET isotope of manganese seems the most promising approach to eliminate these problems and was recently reported [9, 10].

Additionally, radiomanganese can also directly be used for PET studies in its cationic form or in complexed form as new model radiotracers similar to the various  $^{68}\text{Ga}$ -complex tracers available. The beneficial decay properties of short- and longer-lived radioisotopes of manganese available for PET imaging in combination with stable complexes in its bi- and tetra-valent ionic form open a wide range of possibilities for labelling of new tracers with special features.

The decay properties of the most suitable  $\beta^+$ -emitting radioisotopes  $^{51}\text{Mn}$ ,  $^{52m}\text{Mn}$  and  $^{52g}\text{Mn}$  are summarized in Table 1 (taken from Ref. [11]).

\*Corresponding author: Ingo Spahn, Institut für Neurowissenschaften und Medizin, INM-5: Nuklearchemie, Forschungszentrum Jülich, 52425 Jülich, Germany, e-mail: i.spahn@fz-juelich.de

Martin Buchholz, Heinz H. Coenen: Institut für Neurowissenschaften und Medizin, INM-5: Nuklearchemie, Forschungszentrum Jülich, 52425 Jülich, Germany

**Table 1:** Decay properties of the radioisotopes  $^{51}\text{Mn}$  and  $^{52\text{m,g}}\text{Mn}$  [11].

Isotope	Half-life	Decay probability [%]	max. $\beta^+$ -energy [MeV]	$\gamma$ -ray emission [keV] (intensity [%])
$^{51}\text{Mn}$	46.2 min	97 $\beta^+$ 3 EC	2.2	749 (0.26)
$^{52\text{g}}\text{Mn}$	5.59 d	30 $\beta^+$ 70 EC	0.6	744 (90) 935 (95) 1434 (100)
$^{52\text{m}}\text{Mn}$	21.1 min	96.5 $\beta^+$ 1.6 EC 1.8 IT	2.6	378 (1.7) 1434 (98.3)

The production of short-lived  $^{51}\text{Mn}$  was studied in detail in our institute using proton and deuteron induced reactions on  $^{\text{nat}}\text{Cr}$  and enriched  $^{50}\text{Cr}$ , respectively [12–14]. The proton induced production requires energies above 20 MeV while the deuteron induced reaction needs higher effort. The other radionuclide  $^{52\text{m}}\text{Mn}$  is obtained either as a product of the  $^{52}\text{Fe}$  ( $^{52\text{m}}\text{Mn}$ ) generator system [cf. 15] or it is obtained directly *via* a suitable nuclear reaction [16–19]. Its half-life of 21.1 min is, however, rather short.

For synthesis, development and initial imaging studies, the longer-lived radioisotope  $^{52\text{g}}\text{Mn}$  offers itself as the more promising candidate. For its production detailed cross section measurements have been performed [12, 13, 16, 20–24] and the isomeric cross section ratio  $^{52\text{m}}\text{Mn}/^{52\text{g}}\text{Mn}$  was analysed in several reactions [25]. It was shown that protons on  $^{\text{nat}}\text{Cr}$  yield sufficient amounts of  $^{52\text{g}}\text{Mn}$  for imaging applications [23], i.e. in a radionuclidically pure form, provided a waiting time of 4 h is allowed to let the short-lived isotopes decay out.

Reported no-carrier-added separation methods for radiomanganese from the target material chromium [13, 23, 26–28] still need improvement concerning efficacy and handling. Therefore, the focus of this work was on an optimized radiochemical separation to obtain the PET suitable isotope  $^{52\text{g}}\text{Mn}$  more easily in its bi-valent oxidation state for the labelling of molecular probes like  $T_1$  contrast enhancing agents in MRI. Some work on this topic has already been done in our group [9, 29], and a more comprehensive study on the radiolabelling of  $[\text{Mn}^{\text{II}}(\text{CDTA})]^{2-}$  will be published separately [10]. For this purpose a thorough study of distribution coefficients considering different media and exchange resins was done, and the translation of the most promising combination into a column chromatographic method was achieved.

## 2 Materials and methods

### 2.1 Radionuclide production and target processing

The radionuclide  $^{52\text{g}}\text{Mn}$  was produced by irradiation of  $^{\text{nat}}\text{Cr}$  (Goodfellow Ltd., 99.9% purity) with protons. For this, cast chromium plates with a mean area weight of  $0.36 \pm 0.1 \text{ g cm}^{-2}$  were irradiated with protons in the energy range from 16.9 to 8.2 MeV at the Baby Cyclotron BC1710 of INM-5 (Forschungszentrum Jülich) [30]. The simultaneously produced  $^{51}\text{Cr}$  (half-life: 27.7 d) was used to trace the “bulk” target material Cr in both distribution coefficient measurements and subsequent chromatographic separations.

In all experiments the irradiated Cr plates were dissolved overnight in 5 mL conc. HCl (Sigma-Aldrich, ACS reagent) at 70 °C and the solution subsequently evaporated to dryness. The residue was dissolved in 5 mL HPLC-grade  $\text{H}_2\text{O}$  and used as a stock solution for the measurement of distribution coefficients. In case of the chromatographic separation the residue was directly dissolved in the corresponding elution solvent.

### 2.2 Measurement of radioactivity

The  $\gamma$ -ray measurements were conducted with four different ORTEC  $\gamma$ -ray spectrometers (AMETEK GmbH, Berwyn, USA). The distance of different samples to the detector during counting was adjusted between 10 and 50 cm aiming for low dead times. Each detector was calibrated for efficiency and energy with different standard radiation point sources supplied by Amersham (UK) and PTB (Germany).

### 2.3 Determination of distribution coefficients

In order to develop an optimized radiochemical separation of  $^{52\text{g}}\text{Mn}$  from  $^{\text{nat}}\text{Cr}$  a series of measurements on distribution coefficients for an anion (Amberlite CG-400-II<sup>TM</sup>) and a cation exchange resin (DOWEX 50WX8<sup>TM</sup>) with various eluents was performed. Methanol, ethanol, iso-propanol and butanol were investigated as eluents. For this purpose, 50–100 mg of the resin, after drying in an oven overnight, were transferred into a 2 mL Eppendorf reaction vial. The resin was conditioned with 1.5 mL of the respective eluent by shaking the mixture with a vortex wobbler (Vortex-Genie 2, Scientific Industries, New York, USA) for at least 24 h. Aliquots of 50  $\mu\text{L}$  of the previously prepared stock

solution, consisting of  $^{52g}\text{Mn}$ ,  $^{51}\text{Cr}$  and non-radioactive chromium, were then added to the resin-eluent mixture.

Additionally, reference samples were prepared by diluting 50  $\mu\text{L}$  of the same stock solution with the respective eluent. Both were equilibrated for 1 h by shaking. After the liquid-solid separation a 500  $\mu\text{L}$  aliquot was taken from each, the liquid phase of the mixture and of the reference samples. The amounts of radionuclides present in the liquid phase were determined by  $\gamma$ -ray spectrometry, using HPGe-detectors. The reference samples were used to measure the total amount of radioactivity  $A_0$  present in the resin-eluent mixture. The advantage of this reference based method is the reduction of deviations induced by the eventual change of volume of binary solvent mixtures and by differing counting geometries, both leading to smaller or larger values of radioactivity. Finally, the  $K_D$ -value of each system was calculated with the distribution coefficient according to the following equation:

$$K_D = \left( \frac{A_0 - A_{\text{eq}}}{A_{\text{eq}}} \right) \cdot \frac{V_{\text{aliquot}}}{m_{\text{resin}}}$$

with  $A_0$ : total amount of radioactivity in liquid phase before equilibrium,  $A_{\text{eq}}$ : radioactivity in liquid phase in equilibrium,  $V_{\text{aliquot}}$ : volume of measured aliquot in mL,  $m_{\text{resin}}$ : mass of resin in g.

## 2.4 Anion exchange separation of $^{52g}\text{Mn}$ from $^{\text{nat}}\text{Cr}$

The final separation of radiomanganese from bulk chromium was performed using an anion exchange resin (Amberlite CG-400-II, Fluka, Hannover, Germany) which was soaked overnight in acetic acid and methanol (50 : 50). The resin was packed in a chromatography column (10 mm diameter, 50 mm length) with a water heating/cooling mantle and rinsed with tenfold column volume of the eluent (acetic acid/methanol 50 : 50) for conditioning and for removing impurities. After column preparation, the irradiated chromium target weighing  $478 \pm 5$  mg was dissolved in 3 M HCl (5 mL). The acid was evaporated at 130 °C, the residue taken up in the eluent (5 mL) and carefully transferred to the top of the resin. After initial elution of the main, dark green chromium fraction at room temperature the column was heated to 50 °C, following a recommendation given in the literature [13], but adapting it to the given experimental set-up. Remaining chromium was eluted with additional 60 mL acetic acid/methanol 50 : 50, and the radiomanganese was quantitatively eluted afterwards with 3 M hydrochloric acid (3 mL). In the development

experiments each of the collected fractions containing radiomanganese was reduced to dryness at 110 °C to assure suitable counting geometry in all following  $\gamma$ -ray spectroscopic measurements.

The residues were analyzed by  $\gamma$ -ray spectroscopy to monitor the elution profile of the separation method. Each fraction was measured twice with a HPGe-detector. One short measurement of about 30 min was done directly after the separation to assess the  $^{52g}\text{Mn}$  content using its high intensity  $\gamma$ -rays at 744.23 (90.0%), 935.54 (95%) and 1434.07 keV (100%). The chromium content was traced with  $^{51}\text{Cr}$  (half-life: 27.7 d,  $\gamma$ -ray: 320 keV (9.81%)) which was simultaneously produced in the irradiations. After the decay of  $^{52g}\text{Mn}$ , i.e. several weeks later, a long measurement was performed to precisely determine the longer lived radionuclides in the main fractions.

## 2.5 Experimental uncertainties

All experimental results were obtained by relative measurements of radioactivity. Thus mainly the uncertainties of the different counting efficiencies at different sample-detector distances and to a smaller degree those of the counting statistics were relevant. The overall uncertainty based on these factors amounts to 5 to 8%. Volumetric uncertainties faced during sample preparation are below 1% and could be neglected.

# 3 Results and discussion

## 3.1 Radionuclide production

A comprehensive report on the proton induced production of radiomanganese and the resulting radionuclide yields has recently been published by Buchholz et al. [23]. In this work  $^{52g}\text{Mn}$  batches of about 25 to 40 MBq were obtained. The short-lived radioactive co-products  $^{51}\text{Mn}$  and  $^{52m}\text{Mn}$  decayed out during the chemical processing. The long-lived contaminants  $^{53}\text{Mn}$  ( $T_{1/2} = 3.7 \times 10^6$  a) and  $^{54}\text{Mn}$  ( $T_{1/2} = 312.2$  d) were not observed in the  $\gamma$ -ray spectra. Whereas the formation of  $^{53}\text{Mn}$  can be neglected, the formation of the latter one is to be expected. Based on the report of Dmitriev and Molin [31] the co-production of  $^{54}\text{Mn}$  should be less than 0.2% (data taken from EXFOR [32]) and would therefore not interfere with the application of  $^{52g}\text{Mn}$  for medical imaging purposes, and would thus not require use of enriched target material.

### 3.2 Distribution coefficients

The  $K_D$  values of the cation exchange resins in combination with ethanol as eluent, containing the complexing agent DEHP, indicated no sufficient separation factor and are therefore not further discussed here. However, promising results were obtained, using simple alcohols like methanol and ethanol together with the anion exchange resin Amberlite CG-400-II. The respective  $K_D$ -values and separation factors of different alcohols are depicted in Figures 1 and 2.

While the use of an alcohol like methanol already results in a high separation factor of  $1537 \pm 244$ , there is still low chromium absorption evident on the resin. Therefore, another study on suitable  $K_D$ -values was performed, in-

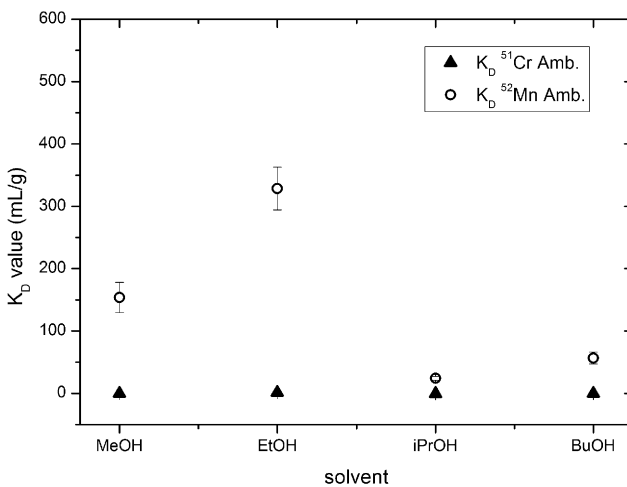


Fig. 1:  $K_D$ -values of  $^{52g}\text{Mn}$  and  $^{51}\text{Cr}$  on Amberlite CG-400-II in combination with different alcohols.

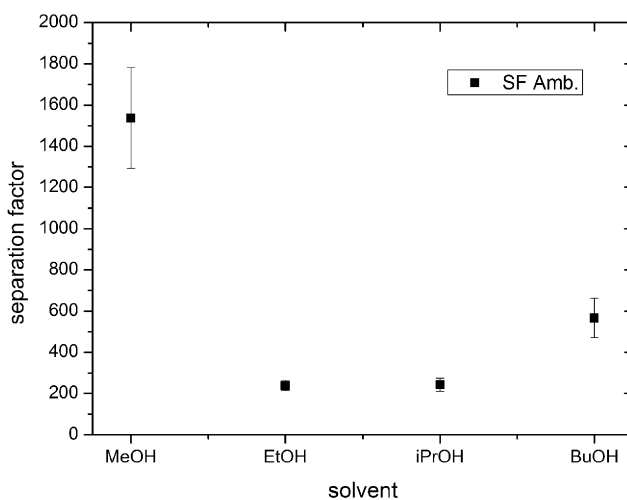


Fig. 2: Separation factors of  $^{52g}\text{Mn}$  from  $^{51}\text{Cr}$  on Amberlite CG-400-II in combination with different alcohols.

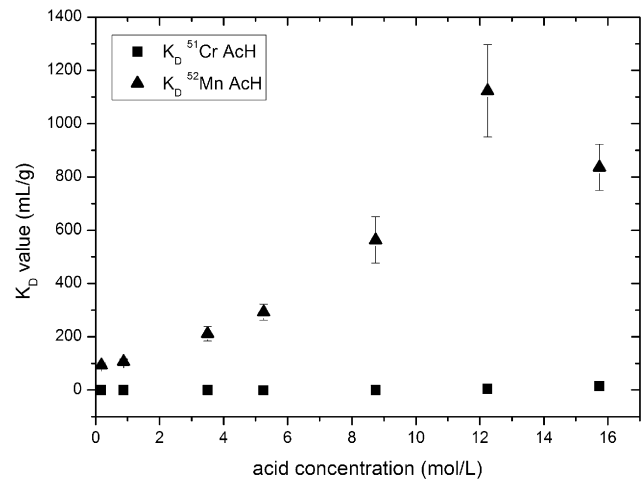


Fig. 3: Effect of acetic acid concentration in methanol on  $K_D$ -value with Amberlite CG-400-II.

vestigating acetic acid as additive to further suppress the chromium retention on the anion exchange resin.

The addition of acetic acid to methanol showed the greatest effect on the ion exchange behaviour of Cr and Mn (see Figure 3). The Mn absorption rises steadily until the acetic acid concentration of 12.24 M is reached. However, at the same concentration a simultaneous absorption of chromium can be observed. Therefore, 8.74 M turned out as optimal acetic acid concentration for a high radiomanganese absorption and low Cr retention, leading to a maximal separation factor of  $5632 \pm 872$ . This corresponds to a 50 : 50 volume mixture of acetic acid and methanol. The optimal parameters determined were then used in a column chromatographic separation.

### 3.3 Anion exchange separation of $^{52g}\text{Mn}$ from $^{nat}\text{Cr}$

Based on the analyses of the eluted fractions the elution profile of the separation system could be compiled. Due to the significantly lower  $^{51}\text{Cr}$  production rate of  $1.60 \pm 0.16 \text{ MBq } \mu\text{A}^{-1} \text{ h}^{-1}$  [23] in comparison to  $^{52g}\text{Mn}$  and due to the lower intensities of the  $^{51}\text{Cr}$   $\gamma$ -rays, the detection limit of  $^{nat}\text{Cr}$  in the fractions was only approximately 0.5 mg. An elution profile of the separation is exemplarily shown in Figure 4. The elevated temperature of the HCl eluent lead to an increased elution of radiomanganese and thus reduced the necessary volume of 3 M HCl.

For further characterization, in the subsequent experiments the radiomanganese containing fractions were combined and the solvent evaporated. The residue of the combined n.c.a.  $^{52g}\text{Mn}$  fractions was dissolved in 200  $\mu\text{L}$

Authors	Separation method	Valence	Final solution	
			Cr-content [%]	Mn-yield [%]
Klein et al. [13]	co-precipitation, solid-phase-extraction	Cr(VI), Fe(III), Mn(IV)	0.03 – 99	10
Lahiri et al. [26]	liquid-liquid-extraction	Cr(III), Mn(II)	< 0.01 60	10
Lewis et al. [27]	anion-exchange	Cr(III), Mn(II)	1.2 60	40–86
Buchholz et al. [23]	cation-exchange	Cr(III), Mn(II)	< 0.1 99	12
This work	anion exchange	Cr(III), Mn(II)	0.02 99.5	2–3

**Table 2:** Comparison of known separation methods of radiomanganese from chromium.

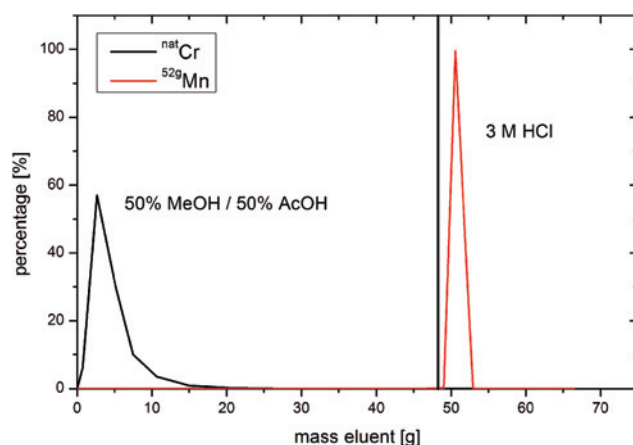


**Fig. 4:** Elution profile of the optimized separation of  $^{52g}\text{Mn}$  from Cr (resin: Amberlite CG400, Cr eluent: 1 : 1 MeOH/AcOH, Mn eluent: 3 M HCl).

of de-ionized water and then analyzed with ICP-MS to measure the exact amount of chromium. The analysis revealed an impurity of 0.07 mg (0.014%) in the n.c.a.  $^{52g}\text{Mn}$  solution. The +2 oxidation state of Mn was additionally confirmed by radio-ion-chromatography (Metrohm 882 Compact IC plus, Metrohm, Switzerland). Thereby, the resulting solution was ready for first labelling experiments without further purification.

### 3.4 Comparison with existing separation methods

It is worth mentioning that several other separation methods have been published so far [13, 23, 26–28] and are summarized in Table 2 for comparison.

The co-precipitation of Mn(IV) with the non-isotopic carrier Fe(III), followed by solid phase extraction and anion-exchange chromatography, as proposed by Klein

et al. [13], provided a 99%  $^{52g}\text{Mn}$  recovery with a Cr impurity as low as 0.03%. However, this method was only optimized for small, inactive Cr amounts of 5 mg and used strong oxidizing agents, requiring the reduction of Mn(IV) back to Mn(II). Another published procedure is based on liquid-liquid extraction of Mn(II) with trioctyl amine [26, 27]. By this technique very pure n.c.a.  $^{52g}\text{Mn}$  samples were obtained with chromium impurities as low as 5.35 ng. The major disadvantage of this technique was later shown by Lewis et al. [27]: repetitions of the process necessary for samples with higher starting Cr contents of 70 mg lead to a relatively low  $^{52g}\text{Mn}$  recovery of only 35%.

A further approach based on an anion exchange separation was initially proposed by Topping et al. [28]. However, they ran only an inactive “mocking” separation to determine the Cr impurity in the final solution. No further data on the amount of the eluent containing  $^{52g}\text{Mn}$  or on actual Cr impurities were given. Then a follow up study by Lewis et al. [27] revealed a high fraction of 1.2% Cr-impurity present in the  $^{52g}\text{Mn}$  solution, a mediocre  $^{52g}\text{Mn}$  recovery and rather large volume fractions of 40–86 mL, making the proposed separation not favorable.

A chromatographic separation of n.c.a.  $^{52g}\text{Mn}$  from macroscopic amounts of  $^{nat}\text{Cr}$  based on the cation-exchange resin DOWEX 50WX8, as previously developed by our group [23], could only be achieved after an extensive removal of chloride ions. Otherwise, the n.c.a.  $^{52g}\text{Mn}$  obtained was contaminated with  $\text{Cr}[(\text{H}_2\text{O})_5\text{Cl}]^{2+}$  complexes [13] which showed an identical retention behavior as  $^{52g}\text{Mn}$ .

Therefore all reported separation methods either showed high Cr impurities, large  $^{52g}\text{Mn}$  elution volumes, or required several experimental steps or repetitions. The new method described here provides a more straightforward approach without complicated processing steps, and hence a higher reproducibility. However, the disadvantage of the new method is clearly the long time needed for the

dissolution of the target and for the ion exchange. For the shorter-lived promising PET radioisotopes  $^{51}\text{Mn}$  and  $^{52\text{m}}\text{Mn}$  this separation could only be efficiently used by shortening of these two steps. While the dissolution of the target might be optimized by physical means such as pulverizing the solid metal target before dissolution, an introduction of a pressurized chromatography method leading to accelerated solvent flow could considerably reduce the time necessary for the separation by ion-exchange.

Presently, for animal testing or even clinical trials a combination of two procedures appears to be the most suitable approach: removal of macroscopic Cr amounts as developed here followed by a fine separation with the optimized trioctyl amine extraction process discussed above.

Further on, by focusing just on the macroscopic removal of chromium, the flow rate in the ion exchange separation can be increased as well as the amount of washing solution can be reduced, both provisions leading to a shorter separation time. If the macroscopic amount of chromium is removed, then more sophisticated liquid-liquid separations with small volumes can efficiently be applied to produce n.c.a. radiomanganese in a much shorter time.

## 4 Conclusion

In search for a new and more facile method for the radiochemical separation of  $^{52\text{g}}\text{Mn}$  from  $^{\text{nat}}\text{Cr}$  for future use, e.g. labelling of  $T_1$  MRI contrast agents, the measurement of distribution coefficients proved an indispensable tool to evaluate the viability of different chromatographic separation systems. Using an acetic acid/methanol 1 : 1 mixture on the anion exchange resin Amberlite CG400, a nearly quantitative absorption of  $^{52\text{g}}\text{Mn}$  was found, with nearly no absorption of  $^{\text{nat}}\text{Cr}$ .

The transfer of the eluent combination into a chromatographic separation method enabled the facile separation of  $^{52}\text{Mn}$  and  $^{\text{nat}}\text{Cr}$  with the anion-exchange resin Amberlite CG400. With this separation system,  $^{\text{nat}}\text{Cr}$  is eluted before  $^{52}\text{Mn}$  with a 1 : 1 mixture of acetic acid/methanol and afterwards n.c.a.  $^{52\text{g}}\text{Mn}$  with 3 M HCl at 50 °C. It yielded 99.5% of n.c.a.  $^{52}\text{Mn}$  in 2–3 mL of 3 M HCl within a separation time of 3–4 h and without the need for an extensive target processing prior to the separation. An ICP-MS analysis revealed a chromium impurity of 0.07 mg (0.014%) in the n.c.a.  $^{52}\text{Mn}$  solution. This amount of chromium is sufficiently low enough for preliminary labeling experiments and PET studies with  $^{52}\text{Mn}$ . However, for future pharmacological test with animals or even for clinical trials, further optimization

to achieve even lower chromium impurities is necessary. For this a combination of the newly developed procedure with an extraction method as discussed above could offer a solution. In this work radionuclide production runs, yielding about 13 MBq of radiomanganese within 1 h and at about 1  $\mu\text{A}$  beam current, were conducted. Upscaling of those experiments can easily be achieved without any major changes to the experimental set-up. However, the transfer of the conditions presented here to an automated system is needed, if amounts of radioactivity above 100 MBq  $^{52}\text{Mn}$  are to be produced and handled. Furthermore, an optimization of the duration of separation is also essential, if the procedure should be utilized for the production of the isotope  $^{51}\text{Mn}$  which is most promising for application with clinical PET.

**Acknowledgement:** The authors would like to thank Prof. Dr. Dr. h.c. mult. S. M. Qaim for very helpful discussions and his constructive advice. Sincere thanks also go to Mr. Holzgreve, Mr. Adrian, and Mr. Spellerberg involved in the cyclotron irradiations and radionuclide production.

## References

1. Cacace, A. T., Brozoski, T., Berkowitz, B., Bauer, C., Odintsov, B., Bergkvist, M., Castracane, J., Zhang, J. S., Holt, A. G.: Manganese enhanced magnetic resonance imaging (MEMRI): a powerful new imaging method to study tinnitus. *Hear. Res.* **311**, 49 (2014).
2. Lin, Y.-J., Koretsky, A. P.: Manganese ion enhanced T1-weighted MRI during brain activation: an approach to direct imaging of brain function. *Magnetic Resonance in Medicine* **38**, 378 (1997).
3. Silva, A. C., Bock, N. A.: Manganese-Enhanced MRI: An exceptional tool in translational neuroimaging. *Schizophr. Bull.*, **34**, 595 (2008).
4. Silva, A. C., Lee, J. H., Aoki, L., Koretsky, A. R.: Manganese-enhanced magnetic resonance imaging (MEMRI): methodological and practical considerations. *NMR Biomed.* **17**, 532 (2004).
5. Michalke, B., Halbach, S., Nischwitz, V.: Speciation and toxicological relevance of manganese in humans. *J. Environ. Monit.*, **9**, 650 (2007).
6. Boretius, S., Frahm, J.: Manganese-enhanced magnetic resonance imaging, in: *In Vivo NMR Imaging: Methods and Protocols*. (Schroder, L., Faber, C., eds.) vol. 531, Humana Press Inc, Totowa, USA (2011).
7. Kueny-Stotz, M., Garofalo, A., Felder-Flesch, D.: Manganese-enhanced MRI contrast agents: from small chelates to nano-sized hybrids. *Eur. J. Inorg. Chem.* **12**, 1987 (2012).
8. Massaad, C. A., Pautler, R. G.: *Manganese-Enhanced Magnetic Resonance Imaging (MEMRI)*. Humana Press Inc, Totowa, USA (2011).
9. Coenen, H. H., Buchholz, M., Spahn, I., Vanasschen, C., Ermer, J., Neumaier, B.: Towards authentically labelled bi-

- modal PET(SPECT)/MR-probes. *EJNMMI Physics* **1**(Suppl. 1), A79 (2014).
10. Vanasschen, C., Brand, M., Ermert, J., Neumaier, B., Coenen, H. H.: Isotopically radiolabelled  $[\text{MnII}(\text{CDTA})]^{2-}$  as stable complex for bimodal PET/MR imaging. *RSC Advances*, submitted.
  11. Chadwick, M. B., Obložinský, P., Herman, M., Greene, M. N., McKnight, R. D., Smith, D. L., Young, P. G., MacFarlane, R. E., Hale, G. M., Frankle, S. C., Kahler, A. C., Kawano, T., Little, R. C., Madland, D. G., Moller, P., Mosteller, R. D., Page, P. R., Talou, P., Trellue, H., White, M. C., Wilson, W. B., Arcilla, R., Dunford, C. L., Mughabghab, S. F., Pritychenko, B., Rochman, D., Sonzogni, A. A., Lubitz, C. R., Trumbull, T. H., Weinman, J. P., Brown, D. A., Cullen, D. E., Heinrichs, D. P., McNabb, D. P., Derrien, H., Dunn, M. E., Larson, N. M., Leal, L. C., Carlson, A. D., Block, R. C., Briggs, J. B., Cheng, E. T., Huria, H. C., Zerkle, M. L., Kozier, K. S., Courcelle, A., Pronyaev, V., van der Marck, S. C.: ENDF/B-VII.0: Next generation evaluated nuclear data library for nuclear science and technology. *Nucl. Data Sheets* **107**, 2931 (2006).
  12. Klein, A. T. J., Rösch, F., Qaim, S. M.: Investigation of Cr-50( $d, n$ )Mn-51 and Cr-nat( $p, x$ )Mn-51 processes with respect to the production of the positron emitter Mn-51. *Radiochim. Acta* **88**, 253 (2000).
  13. Klein, A. T. J., Rösch, F., Coenen, H. H., Qaim, S. M.: Production of the positron emitter  $^{51}\text{Mn}$  via the  $^{50}\text{Cr}(d, n)$  reaction: targetry and separation of no-carrier-added radiomanganese. *Radiochim. Acta* **90**, 167 (2002).
  14. Klein, A. T. J., Rösch, F., Coenen, H. H., Qaim, S. M.: Labelling of manganese-based magnetic resonance imaging (MRI) contrast agents with the positron emitter  $^{51}\text{Mn}$ , as exemplified by manganese-tetraphenyl-porphin-sulfonate (MnTPPS4). *Appl. Radiat. Isot.* **62**, 711 (2005).
  15. Qaim, S. M.: Cyclotron production of generator radionuclides. *Radiochim. Acta* **41**, 111 (1987).
  16. Wing, J., Huizenga, J. R., ( $p, n$ ) cross sections of V-51, Cr-52, Cu-63, Cu-65, Ag-107, Ag-109, Cd-111 and La-139 from 5 to 10.5 MeV. *Phys. Rev.* **128**, 280 (1962).
  17. Barrandon, J. N., Debrun, J. L., Kohn, A., Spear, R. H., Study of level of Ti, V, Cr, Fe, Ni, Cu and Zn by activation with protons whose energy is limited to 20 MeV. *Nuclear Instruments Methods* **127**, 269 (1975).
  18. Muminov, V. A., Mukhammedov, S., Vasidov, A., Possibilities of proton-activation analysis for determining the content of elements from short-lived radionuclides. *Soviet Atomic Energy* **49**, 540 (1980).
  19. Skakun, E. A., Batii, V. G., Rakivnenko, Y. N., Rastrepin, O. A.: Investigation of Cr-52( $p, n$ )Mn-52m,g and Cr-54( $p, n$ )Mn-54 reaction cross section in the 5–9 MeV energy range. *Izvestiya Akademii Nauk Sssr Seriya Fizicheskaya* **50**, 2043 (1986).
  20. West, H. I., Lanier, R. G., Mustafa, M. G.: (Cr-52( $p, n$ )Mn-g,m)-Mn-52 and (Cr-52( $d, 2n$ )Mn-g,m)-Mn-52 excitation-functions. *Phys. Rev. C* **35**, 2067 (1987).
  21. Levkovskij, V. N., Activation Cross Sections for the Nuclides of Medium Mass Region ( $A = 40-100$ ) with Medium Energy ( $E=10-50$  MeV) Protons and Alpha Particles (Experiment and Systematics). Inter-Vesi, Moscow, Russia (1991).
  22. Zaman, M. R., Spellerberg, S., Qaim, S. M.: Production of  $^{55}\text{Co}$  via the  $^{54}\text{Fe}(d, n)$ -process and excitation functions of  $^{54}\text{Fe}(d, t)^{53}\text{Fe}$  and  $^{54}\text{Fe}(d, \alpha)^{52m}\text{Mn}$  reactions from threshold up to 13.8 MeV. *Radiochim. Acta* **91**, 105 (2003).
  23. Buchholz, M., Spahn, I., Scholten, B., Coenen, H. H.: Cross-section measurements for the formation of manganese-52 and its isolation with a non-hazardous eluent. *Radiochim. Acta* **101**, 491 (2013).
  24. Wooten, A. L., Lewis, B. C., Lapi, S. E.: Cross-sections for ( $p, x$ ) reactions on natural chromium for the production of  $^{52,52m,54}\text{Mn}$  radioisotopes. *Appl. Radiat. Isot.* **96**, 154 (2015).
  25. Qaim, S. M., Sudár, S., Fessler, A.: Influence of reaction channel on the isomeric cross-section ratio. *Radiochim. Acta* **93**, 503 (2005).
  26. Lahiri, S., Nayak, D., Korschinek, G.: Separation of no-carrier-added Mn-52 from bulk chromium: a simulation study for accelerator mass spectrometry measurements of Mn-53. *Anal. Chem.* **78**, 7517 (2006).
  27. Lewis, C. M., Graves, S. A., Hernandez, R., Valdovinos, H. F., Barnhart, T. E., Cai, W. B., Meyerand, M. E., Nickles, R. J., Suzuki, M.: Mn-52 production for PET/MRI tracking of human stem cells expressing divalent metal transporter 1 (DMT1). *Theranostics* **5**, 227 (2015).
  28. Topping, G. J., Schaffer, P., Hoehr, C., Ruth, T. J., Sossi, V.: Manganese-52 positron emission tomography tracer characterization and initial results in phantoms and in vivo. *Medical Physics* **40**, 4 (2013).
  29. Vanasschen, C., Brand, M., Ermert, J., Neumaier, B., Coenen, H. H.: Authentically radiolabelled Mn(II) complexes as bimodal PET/MR tracers. *EJNMMI Physics* **2**(Suppl 1), A85 (2015).
  30. Spellerberg, S., Scholten, B., Spahn, I., Bolten, W., Holzgreve, M., Coenen, H. H., Qaim, S. M.: Target development for diversified irradiations at a medical cyclotron, *Appl. Radiat. Isot.* **104**, 106 (2015).
  31. Dmitriev, P. P., Molin, G., A.: Vop. At. Nauki i Tekhn., Ser. Yadernye Konstanty **5**(44), 43 (1981), Russia.
  32. IAEA-NDS, 2013. Experimental Nuclear Reaction Data (EXFOR). <http://www.nndc.bnl.gov/exfor/exfor00.htm>.